metals

MDPI

Article

Development of Heat Treatments for Structural Parts in Aluminium Alloys Produced by High-Pressure Die Casting (HPDC)

Rui Gomes [1], Gonçalo Soares [1,*], Rui Madureira [1], Rui Pedro Silva [1], José Silva [1], Rui Neto [1,2], Ana Reis [1,2] and Cristina Fernandes [3]

[1] INEGI—Institute of Science and Innovation in Mechanical and Industrial Engineering, Rua Dr. Roberto Frias, 4200-465 Porto, Portugal; rdmadureira@inegi.up.pt (R.M.); rpsilva@inegi.up.pt (R.P.S.); rneto@inegi.up.pt (R.N.); arlr@fe.up.pt (A.R.)

[2] Department of Mechanical Engineering, Faculty of Engineering, University of Porto, Rua Dr. Roberto Frias, 4200-465 Porto, Portugal

[3] Palbit S.A., Rua das Tílias S/N, 3850-582 Albergaria-a-Velha, Portugal; cfernandes@palbit.pt

* Correspondence: gsoares@inegi.up.pt; Tel.: +351-229-578-710

Abstract: In this work, we intended to study the effect of heat treatments (T5 and flash T6) on blistering, mechanical properties and microstructure for different parts produced by vacuum-assisted HPDC. These parts were produced with primary and secondary aluminium alloys (AlSi10MnMg alloy and AlSi10Mg(Fe) alloy, respectively). The parts presented blisters for all combinations of temperature (between 360 °C and 520 °C) and stage times (15 and 30 min) of solution heat treatments. However, when subjected to the T5 heat treatment, blisters were no longer visible. With this heat treatment, there was an increase in yield strength of 64% for both aluminium alloys and an increase in UTS of 31% in AlSi10Mg(Fe) alloy and of 24% in AlSi10MnMg alloy, when compared to the mechanical properties in the as-cast state. However, there was a decrease in ductility. The AlSi10Mg(Fe) alloy presented a lot of contaminations (especially iron), which impaired the mechanical properties compared to the primary aluminium alloy, AlSi10MnMg.

Keywords: vacuum-assisted HPDC; aluminium alloy; T6 heat treatment; T5 heat treatment; flash heat treatment; blistering; automotive industry

Citation: Gomes, R.; Soares, G.; Madureira, R.; Silva, R.P.; Silva, J.; Neto, R.; Reis, A.; Fernandes, C. Development of Heat Treatments for Structural Parts in Aluminium Alloys Produced by High-Pressure Die Casting (HPDC). *Metals* **2024**, *14*, 1059. https://doi.org/10.3390/met14091059

Academic Editor: Srecko Stopic

Received: 28 August 2024
Revised: 13 September 2024
Accepted: 13 September 2024
Published: 16 September 2024

1. Introduction

Aluminium is the second most used metal in the world and is the first in demand in terms of non-ferrous metal, with 75% of aluminium alloys being obtained from ore (primary) and the remaining 25% being produced from recycled aluminium alloys (secondary) [1,2].

Aluminium alloys are increasingly finding application in both the industrial and transportation sectors as an energy-efficient solution, for weight reduction, and to reduce carbon emissions. In North America, the automotive industry has dramatically increased the use of aluminium from 38 kg per car in 1975 to 208 kg in 2020 and 259 kg predicted for 2030, with most of the aluminium parts used being produced by casting. The manufacture of light alloys has seen a substantial increase across the board, but metal casting has witnessed the most remarkable expansion [3].

The interesting features of aluminium alloys, such as their low density, good corrosion resistance, relative ease of recycling, good thermal conductivity, high strength/stiffness-to-weight ratio, and good formability and castability, may justify the rise in consumption over time [4–7].

The concept of the circular economy presents valuable opportunities for optimizing material use by promoting reutilization and resource recycling. This approach minimizes waste in production processes and extends products' lifespans, in contrast to the linear

economy's propensity to squander valuable resources. The goal of transitioning to a circular economy is to slow down the use of finite natural resources, minimize environmental damage from the extraction of raw materials, and minimize pollution from material processing, use, and recycling of end-of-life (EOL) materials [4].

Since manufacturing secondary alloys through recycling results in much lower emissions than the production of primary alloys, material recirculation substantially enhances their potential for reducing CO_2 emissions. Therefore, the circular economy concept is compatible with resources like aluminium, if we consider that, for instance, more than 90% of the aluminium content that is used to produce a car is recycled [4].

The automobile body structures require the best mechanical properties because they are the structural parts subjected to high stress values. It is vital to absorb as much energy as possible in the case of an accident, which demands higher tensile strength along with greater ductility and toughness. However, there are other applications for structural parts produced by high-pressure die-casting, such as marine applications, motorbikes, or structures for recreational vehicles.

Casting alloys to be used in structural components must present a set of characteristics, such as good weldability and rivetability; have high fatigue strength and energy absorption capacity; preferably, they should not require heat treatment; excellent ductility (10–15% elongation); a yield strength value of at least 150 MPa; an ultimate tensile strength value of 300 MPa; and good corrosion resistance [8–10].

Alloy properties and cost are two main issues concerning the above specifications. The use of HPDC to quickly achieve mass production and thus reduce the component cost is a known technique for economic control [11].

In a highly repetitive manufacturing process known as high-pressure die casting (HPDC), molten metal is injected into a mould at high pressure and velocity. With tolerances of $\pm$0.10 mm in 25 mm or $\pm$0.52 mm in 300 mm for aluminium alloys, the parts produced by this method typically have excellent dimensional accuracy and low roughness (0.4 to 3.2 µm). With this process, it is possible to achieve wall thicknesses of approximately 0.6 to 0.9 mm for surfaces with small areas and 2 to 3 mm for surfaces with large areas. The components produced have a fine microstructure, favouring an increase in mechanical strength, due to the rapid injection and cooling speed. The key characteristic that sets this casting process apart from the others is the speed at which the mould is filled and the high pressure applied in the final phase of the injection [12–14].

This process requires a substantial initial investment in equipment, in addition to the expensive and time-consuming development of the complex moulds. HPDC is appropriate when the production series is considerably large (around 100,000 parts), which allows a significant price per part reduction, when accounting for the initial investment of machines, systems and moulds. Additionally, high levels of porosity are inevitable, which drastically reduces the parts' mechanical properties. The use of heat treatments on these parts is problematic due to the considerable high level of porosity, since conventional treatments distort the parts and expand the pores to the surface, ruining the product. This phenomenon is known as blistering [12].

However, performing the necessary heat treatments to obtain the required mechanical properties is possible by means of vacuum assistance during the injection. Vacuum-assisted HPDC involves filling the mould cavity after exhausting the air inside, allowing better metal compaction due to the reduced porosity, resulting in parts with better mechanical properties.

Nevertheless, the high cost of manufacturing will also be reflected in the final product price, despite all the benefits that the vacuum system may provide. This procedure is used only when components of exceptional quality are required, such as structural applications for the automotive sector.

To improve the mechanical properties of Al alloys, heat treatments play a significant role in adjusting several characteristics, including the precipitates' morphology, grain size and removal of residual stresses.

The T5 (artificially aged from the "as-cast" condition) and T6 (solution heat-treated, quenched and artificially aged) heat treatments are commonly applied to aluminium alloys in the 3xx.x series, typically in permanent mould casting and sand casting [15].

The aluminium alloy should be heated to a level just below the eutectic temperature to undergo the solution heat treatment. Strict temperature control is required due to the treatment's harsh conditions, which may cause localised melting of parts, destroying them. On the other hand, heating too far below the eutectic temperature might cause problems, as not all the elements can be dissolved. A solution heat treatment's stage time should be sufficient to produce a dissolution of the hardening elements into the aluminium matrix and a homogenous structure. During this stage, there is also the spheroidization of the silicon particles (change in the morphology of the eutectic silicon) [1,16,17]. After solution heat treatment, parts must be immediately quenched in order to obtain a supersaturated solid solution [1,16,17].

During solution heat treatment, the pressure will rise to a point where it exceeds the elastic limit stress of the material on the porosity walls, irreversibly deforming it, if the temperature or exposure duration is high enough. It should also be noted that when temperature rises, the material's yield strength dramatically decreases. When these phenomena occur, defects can take the shape of small blisters on the part surface [18].

According to Rheinfelden Alloys [19], for Silafont-36 (AlSi10MnMg), the solution heat treatment should be performed between 480 °C and 490 °C for two to three hours, while in special components, it could be performed at 400 °C for 30 min. Other studies investigate this subject even further. In [20], a new T6 heat treatment at 540 °C for 10 min was established. This resulted in a yield strength above 300 MPa and elongation over 2%. A different study in [21] obtained maximum yield strength and ultimate tensile strength with a solution heat treatment of 520 °C for 90 min. Kang et al. [22] investigated the influence of temperature during solution heat treatment, between 480 °C and 540 °C. It was concluded that with the increase in solution heat treatment temperature, there is an improvement in the mechanical properties, where the maximum R_m and $R_{p0.2}$ were obtained under 520 °C for 90 min. However, the intensified porosity expansion during the solution heat treatment at 540 °C for 90 min was detrimental to the mechanical properties.

Aging is one of the most crucial steps in the process of hardening aluminium alloys. A range of mechanical properties can be achieved by adjusting the stage time and temperature, including an increase in yield strength, ultimate tensile strength and hardness, a decrease in residual stresses and stabilisation of the microstructure. Most aluminium alloys start aging immediately after quenching, so it is important to keep the components at low temperatures to prevent any changes in their characteristics before beginning the actual treatment. Artificial aging, which occurs at above room temperatures, often between 90 °C and 250 °C, is distinct from natural aging, which occurs at room temperature [16].

Maximum aging defines the point at which mechanical strength and hardness are at their highest. From this point, an over-aging occurs, in which the precipitates develop more than the ideal, resulting in a decrease in hardness and mechanical strength.

The ability to achieve a significant increase in mechanical strength in the aluminium alloys used in HPDC through heat treatments imposes higher costs. A rapid or flash heat treatment denotes that it will be a treatment of short periods, reducing the thermal cycle length and allowing significant energy savings when compared to conventional heat treatments.

Due to the reduced solution heat treatment duration, it has been estimated from industrial trials that the cost of a flash T6 treatment is about 50% of a conventional treatment for other casting alloys. The costs associated with this treatment correspond to one-third of the solution heat treatment costs and the remaining corresponds to the artificial aging. The energy can be decreased even more if significant time reductions in hardening cycles can be made [23].

The aim of this work is to identify the best heat treatment (T5 or flash T6) for parts injected in aluminium alloys where the vacuum in the moulding cavity is not the most

effective. It is intended to evaluate the optimum combination of parameters (temperature and stage time) of the T6 heat treatment that avoids the appearance of blisters. The T6 heat-treated parts will be compared with the T5 heat-treated parts. With this work, we hope to understand whether a flash T6 heat treatment or whether T5 heat treatment is an alternative to a T6 heat treatment for improving the mechanical properties of parts without material waste caused by blistering.

2. Materials and Methods

2.1. Chemical Composition of the Aluminium Alloys

The chemical composition analysis of the parts was obtained in a previous work [24] with an Ametek SPECTROMAXx (SPECTRO, Kleve, Germany) using arc/spark optical emission spectrometry (OES) and may be found in Table 1.

Table 1. Chemical composition of AlSi10MnMg (1) and AlSi10Mg(Fe) alloy (2) (weight in %).

	Si	Fe	Cu	Mn	Mg	Zn	Ti	Sr	P	Sn	Pb	Ni	Al
1	11.1	0.13	0.001	0.6	0.25	0.001	0.04	0.01	0.001	-	-	-	87.82
2	10.6	0.88	0.14	0.09	0.2	0.05	0.04	-	-	0.001	0.01	0.01	87.97

2.2. Component under Study

A power electronics casing was studied. This casing was produced in two batches of different aluminium alloys, being AlSi10MnMg (primary alloy) and AlSi10Mg(Fe) (secondary alloy), with compromised dimensions of 184 × 126 mm and an average thickness of 2.6 mm—Figure 1.

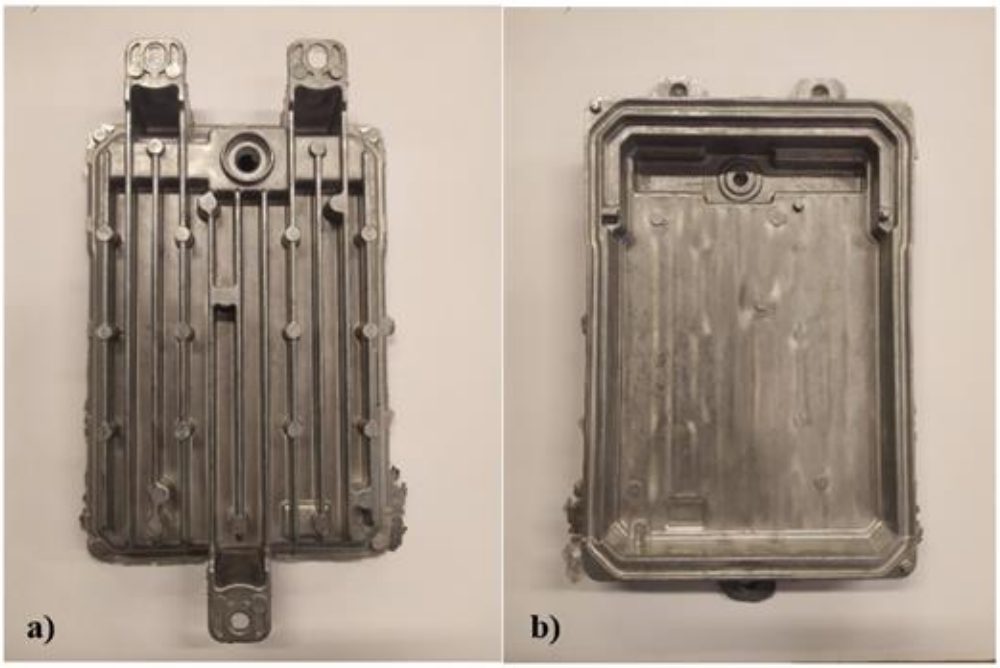

Figure 1. Power electronics casing: (**a**) top view of the part, (**b**) bottom view of the part.

The component was produced on a 400-ton Colosio (Colosio, Botticino Sera, Italy) cold-chamber machine connected to a Fondarex (Fondarex, Switzerland) vacuum system. The vacuum level was regulated for 200 mbar. The remaining main injection parameters are shown in Table 2. The mould temperature was measured after being opened (post-injection) with an infrared camera.

Table 2. Main injection parameters.

Average velocity in gates during the filling phase [m/s]	30–35 (*)
Pouring temperature [°C]	670
Die temperature [°C]	145–220
Vacuum pressure [mbar]	200

* These velocities were obtained in the ProCAST software (2022.0).

2.3. Blistering Study

The aim of this work was to improve the mechanical properties of the injected parts and, simultaneously, to prevent blistering. Different T6 (solution heat treatment followed by artificial aging) and T5 (artificially aged from the as-cast condition) heat treatments were carried out to find the optimum temperature and time parameters.

The heat treatments were performed in an M.J Amaral (M.J.Amaral-Equipamentos Industriais Lda, Vale de Cambra, Portugal) forced convection furnace with the following chamber dimensions: 600 × 600 × 700 mm^3. The interior of this chamber has a double stainless-steel wall to protect the parts from direct radiation.

The temperatures used for the solution heat treatments were based on [19–22], while flash heat treatments (shorter times) were chosen to prevent the appearance of blisters.

Table 3 shows the solution heat treatments performed. In each heat treatment, three parts of AlSi10MnMg alloy were used to compare the number of blisters between them.

Table 3. Solution heat treatments during blistering study.

Solution Heat Treatment No.	Temperature [°C]	Time [min]
1	480	15
2		30
3	470	15
4		30
5	460	15
6		30
7	450	15
8	400	
9	380	
10	360	

Solution heat treatments below 400 °C were performed to prevent blistering. For temperatures far below the eutectic temperature (577 °C), the alloy's response to the solution heat treatment is diminished. Reducing the temperature from 400 °C to 360 °C does not significantly reduce the dissolution of Mg_2Si in the α-Al matrix (from 0.5% at 400 °C to 0.4% at 360 °C). Thus, it is preferred to use a temperature of 360 °C to prevent blistering.

2.4. T6 Heat Treatments

The parameters (temperature and time) for the T6 heat treatment used in this work to study the hardness throughout aging time, were selected based on the results obtained during the blistering study and the studies conducted by [19,21,22].

Table 4 shows the T6 heat treatments for both aluminium alloys (AlSi10MnMg and AlSi10Mg(Fe)). Two parts of each aluminium alloy were used in each heat treatment (different parts for each test).

Due to the low temperature used, in solution heat treatment No. 2, the treatment time was increased to 30 min for compensation of the Mg and Si dissolution reduction. Considering the information given in [19], the time between solution heat treatment and the artificial aging should be less than 12 h. Thus, T6 heat treatment steps (solution heat treatment and artificial aging) were carried out at an interval of less than 12 h.

Table 4. T6 heat treatments selected for this work.

Part No.	Solution Heat Treatment			Artificial Aging	
	No.	Temp. [°C]	Time [min]	Temp. [°C]	Time [h]
1–2	1	520	15	180	2
3–4					3
5–6					4
7–8					5
9–10					6
11–12					7
13–14					8
15–16	2	360	30	180	2
17–18					3
19–20					4
21–22					5
23–24					6
25–26					8

2.5. T5 Heat Treatments

For comparison, two T5 heat treatments (one for each aluminium alloy) were performed with an artificial aging at 180 °C and stage time equal to the stage time at peak age hardening obtained in the T6 heat treatments for each aluminium alloy used. For each T5 heat treatment, three parts were tested. The parts used in the T5 heat treatment were placed in a freezer after injection to prevent natural aging.

2.6. Hardness Measurements

Brinell hardness (HBW 2.5/31.25, which corresponds to HB5) measurements were performed in an EMCO M4U-075 hardness tester (EMCO-Test, Kuchl, Austria). For each heat treatment, each part was tested, at least, in three distinct points in the bottom view of the part, avoiding blister zones. The average hardness and the standard deviation were calculated considering the measurements made in both parts from each alloy under study.

2.7. Microstructural Analysis

A microstructure and defect analysis was carried out using an Olympus PMG 3 optical microscope (Olympus, Tokyo, Japan) with a Leica DP12 digital camera (Leica, Wetzlar, Germany). The microstructure was analysed on eight samples. For each aluminium alloy used in this work, a sample was taken from a part in the as-cast state. Another sample was taken after the T6 heat treatment at peak age hardening and after 8 h of artificial aging, as well as after the T5 heat treatment.

Due to the typical microstructural refinement of the injected alloys, identifying typical structures in the images observed in the optical microscope presented a significant challenge. Thus, for a better characterisation of the microstructure, an FEI Quanta 400FEG ESEM high-resolution scanning electron microscope (SEM) (FEI Company, Hillsboro, OR, USA) was used together with an EDAX Genesis X4M instrument for energy-dispersive X-ray spectroscopy microanalysis (EDS) (Oxford Instruments, Oxfordshire, UK).

2.8. Tensile Tests

Specimens for tensile testing follow the guidelines of ASTM B557M-15 [25]. These specimens were used to determine the mechanical properties of AlSi10MnMg and AlSi10Mg(Fe) alloys after the T5 heat treatments. These specimens were obtained by machining three parts of each alloy used in the T5 heat treatments. Figure 2 shows the positioning of the specimens in the part.

The tensile tests were performed at room temperature on an MTS 810 (MTS, MN, Eden Prairie, MN, USA) equipment with a 10 KN load cell, at a strain rate of 1 mm/min and

with an acquisition frequency of 15 Hz. An MTS (MTS, MN, USA) strain gauge was also used to measure the specimens' deformation.

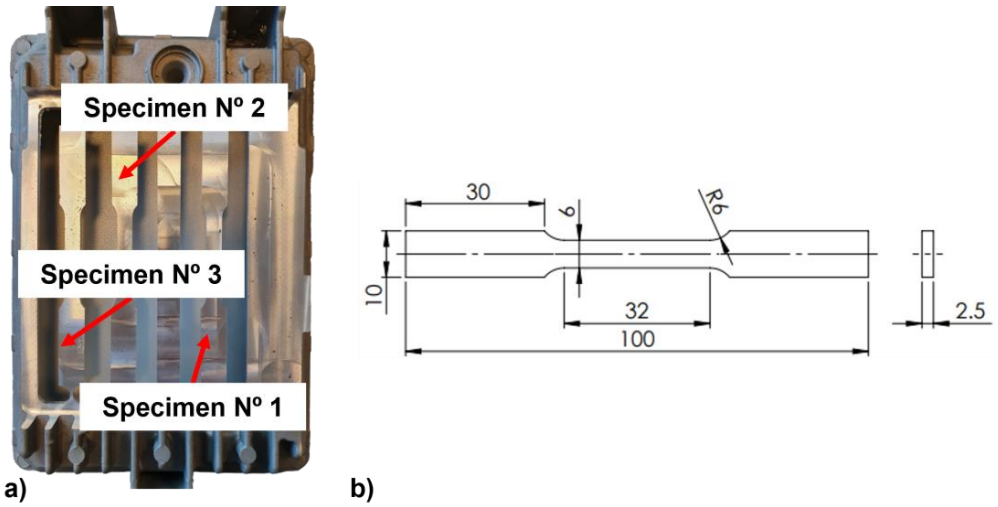

Figure 2. (**a**) Positioning of the specimens on the part, (**b**) Subsize specimen dimensions in millimetres.

3. Results and Discussion

3.1. Blistering

For the same solution heat treatment temperature, varying the cycle time leads to no results for blistering reduction. However, an increase in solution heat treatment temperature, while maintaining the cycle time, leads to an increase in the number and size of blisters.

Table 5 shows the total number of blisters in each part, the average number of blisters and the standard deviation for solution heat treatments over a period of 15 min. After each solution heat treatment, the parts were cleaned and dried so that no contamination could influence the counting of the number of blisters. The parts were visually inspected and the number of blisters was counted by hand by one of the authors of the article.

Table 5. Blistering results for solution heat treatments with a duration of 15 min.

Part No.	Temperature [°C]						
	360	**380**	**400**	**450**	**460**	**470**	**480**
1	3	1	5	27	75	60	65
2	2	10	6	52	60	98	171
3	1	2	7	65	84	112	90
Average	2	4	6	48	73	90	109
St. deviation	1	4	1	16	10	22	45

Figure 3 shows the curve that best fits the evolution of the number of blisters for the different solution heat treatments performed with the same stage time of 15 min.

With the increase in temperature between 360 °C and 480 °C, the blisters' number increases almost exponentially (Figure 4), as concluded in [22]. In general, the standard deviation also increases with increasing solution heat treatment temperature. This highlights a high level of porosity in the parts, which becomes more visible with increasing solution heat treatment temperature.

Part No. 2 at 480 °C has more than twice the number of blisters than part No. 1 at the same solution heat treatment temperature (from 171 to 65 blisters, respectively). The same situation occurs between parts No. 1 and No. 3 at 470 °C (from 60 to 112 blisters, respectively). This evidence a low reproducibility of the casting process, since such a large discrepancy in results is not expected.

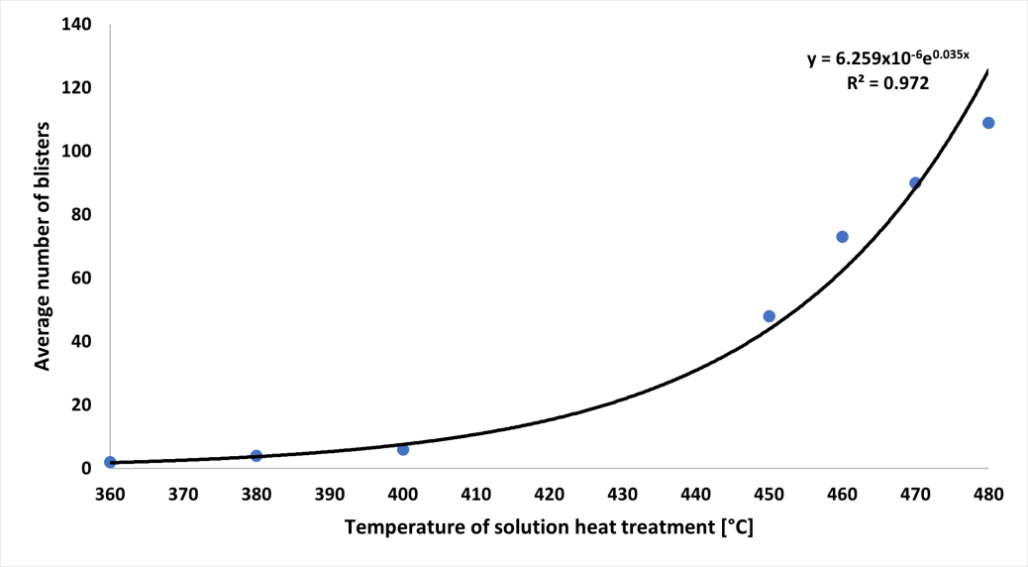

Figure 3. Blistering evolution with solution heat treatment temperature between 360 °C and 480 °C for 15 min.

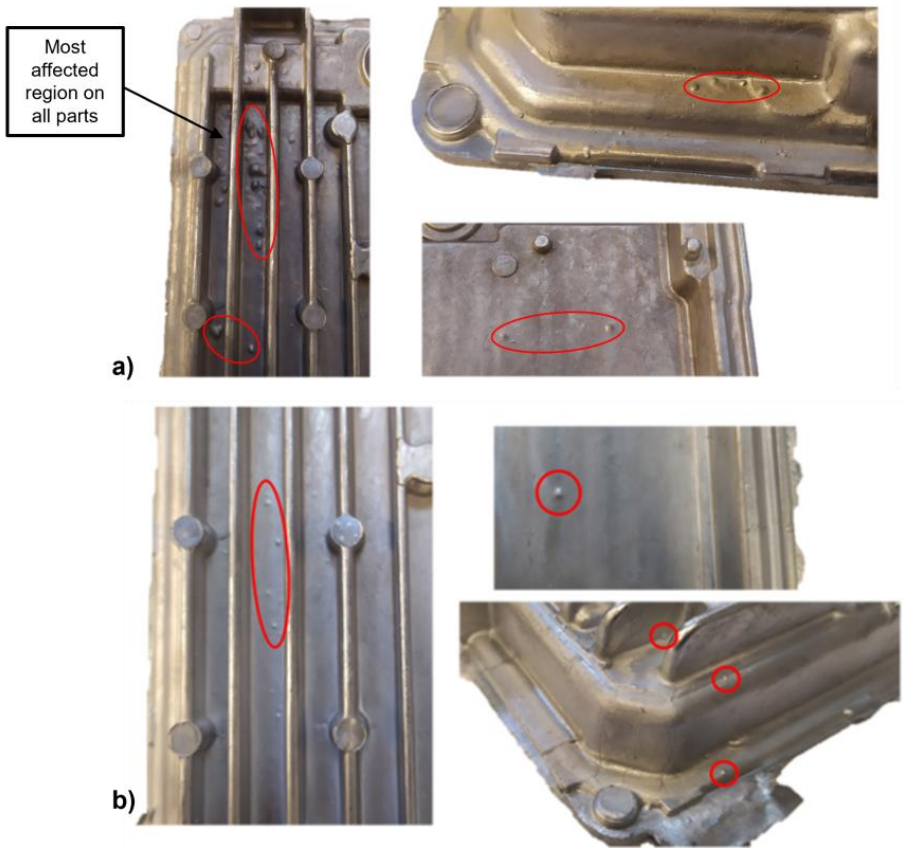

Figure 4. Blistering on the parts: (**a**) Solution heat treatment at 480 °C for 15 min; (**b**) Solution heat treatment at 450 °C for 15 min.

3.2. T6 Heat Treatments

The hardness average values and the respective standard deviations were calculated for the parts in the as-cast state and after the T6 heat treatment (Tables 6 and 7). Figure 5 shows the hardness curve for both alloys for heat treatment No. 1.

Table 6. Hardness results for heat treatment No. 1.

Solution Heat Treatment No. 1–520 °C for 15 min				
Artificial Aging at 180 °C	**Hardness [HB]**			
	AlSi10MnMg		**AlSi10Mg(Fe)**	
Time [h]	**Average**	**St. Deviation**	**Average**	**St. Deviation**
0 (*)	70	2.98	67	3.54
2	95	3.74	90	3.40
3	101	2.98	94	4.20
4	98	3.25	97	3.38
5	98	4.58	100	2.52
6	97	4.23	89	1.52
7	92	2.87	92	1.14
8	91	3.03	87	2.14
As-cast	86	2.15	92	2.64

* After solution heat treatment.

Table 7. Hardness results for heat treatment No. 2.

Solution Heat Treatment No. 2–360 °C for 30 min				
Artificial Aging at 180 °C	**Hardness [HB]**			
	AlSi10MnMg		**AlSi10Mg(Fe)**	
Time [h]	**Average**	**St. Deviation**	**Average**	**St. Deviation**
0 (*)	73	0.98	77	1.31
2	72	0.56	78	0.57
3	73	0.98	78	1.41
4	72	0.68	77	0.83
5	74	1.35	79	1.44
6	73	0.55	78	1.29
8	73	0.38	77	0.83
As-cast	86	2.15	92	2.64

*: After solution heat treatment.

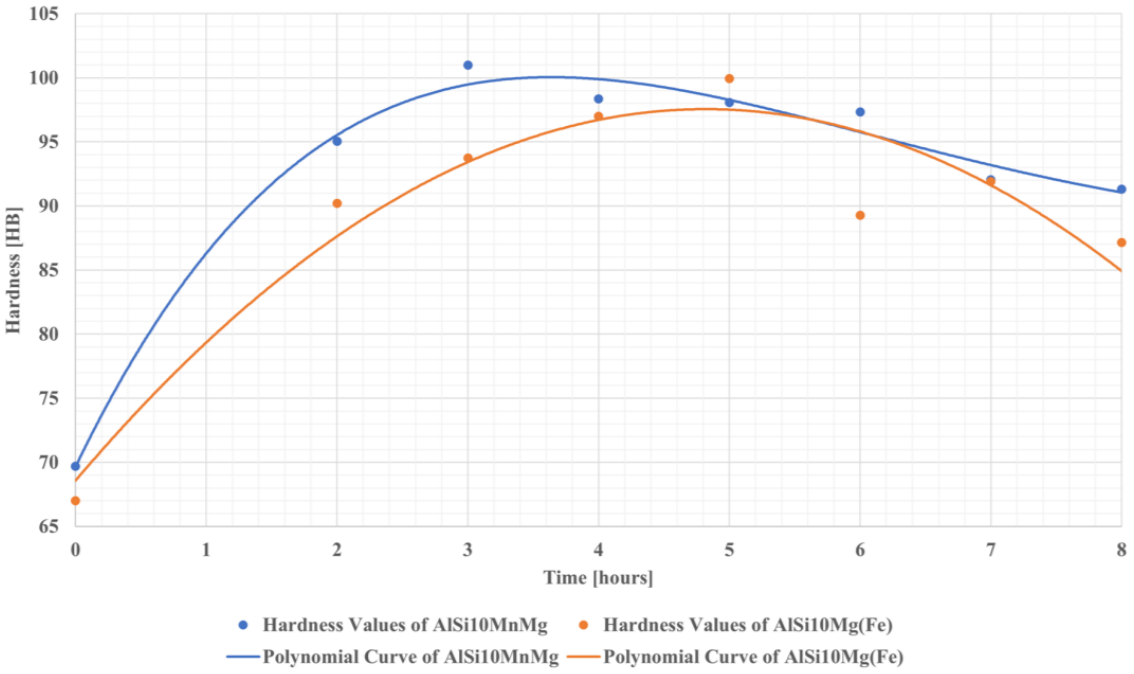

Figure 5. Hardness curves for heat treatment No. 1.

Both aluminium alloys responded to the heat treatments applied. After the solution heat treatment (0 h in the graph of Figure 5), both alloys had a decrease in hardness compared to the as-cast state. This was already expected due to the dissolution of the hardening elements in the aluminium matrix. For both alloys, with increasing time of artificial aging, it is possible to observe a hardness increase. This was the result of the precipitation of the hardening elements. For AlSi10MnMg alloy parts, the peak age hardening occurs at 3 h. The hardness values obtained are in accordance with the Rheinfelden producer, which is stated in [26], values between 90 HB and 110 HB. After this peak, over-aging occurs, resulting in a hardness decrease. At the beginning of the aging process, decomposition of the supersaturated solid solution occurs. Separated Mg and Si clusters are initially formed, and after the diffusion of these atoms, spherical GP (Guinier–Preston) zones appear, which are composed of coherent precipitates. These zones are easily deformed by dislocations leading to localized distortions in the solid solution network. With continued diffusion of the solute into the agglomerates, the GP zones become elongated and give rise to β″ phase precipitates, composed of Mg_5Si_6 with approximately 20% aluminium and a Mg/Si ratio very close to one. Due to the coarser size of this phase, they act as an obstacle to dislocation deformation, contributing to an increase in mechanical strength. If the stage time is prolonged, the β″ phases transform into β′ phases (phase semi-coherent with the matrix) with the composition Mg_2Al. The final phase to form is the β phase (phase incoherent with the matrix), composed of Mg_2Si. As the β″→β′→β transformation takes place, there is a drop in hardness and mechanical strength. For AlSi10Mg(Fe) alloy parts, the peak age hardening happens later, at 5 h of artificial aging. This delay could be attributed to the presence of iron within the alloy, which occupies spaces in the aluminium matrix, preventing precipitates from growing. As happened with the AlSi10MnMg alloy, after the peak age hardening, over-aging occurs, and there is a decrease in hardness. All parts had blisters. Figure 6 shows the hardness curve for both alloys for heat treatment No. 2.

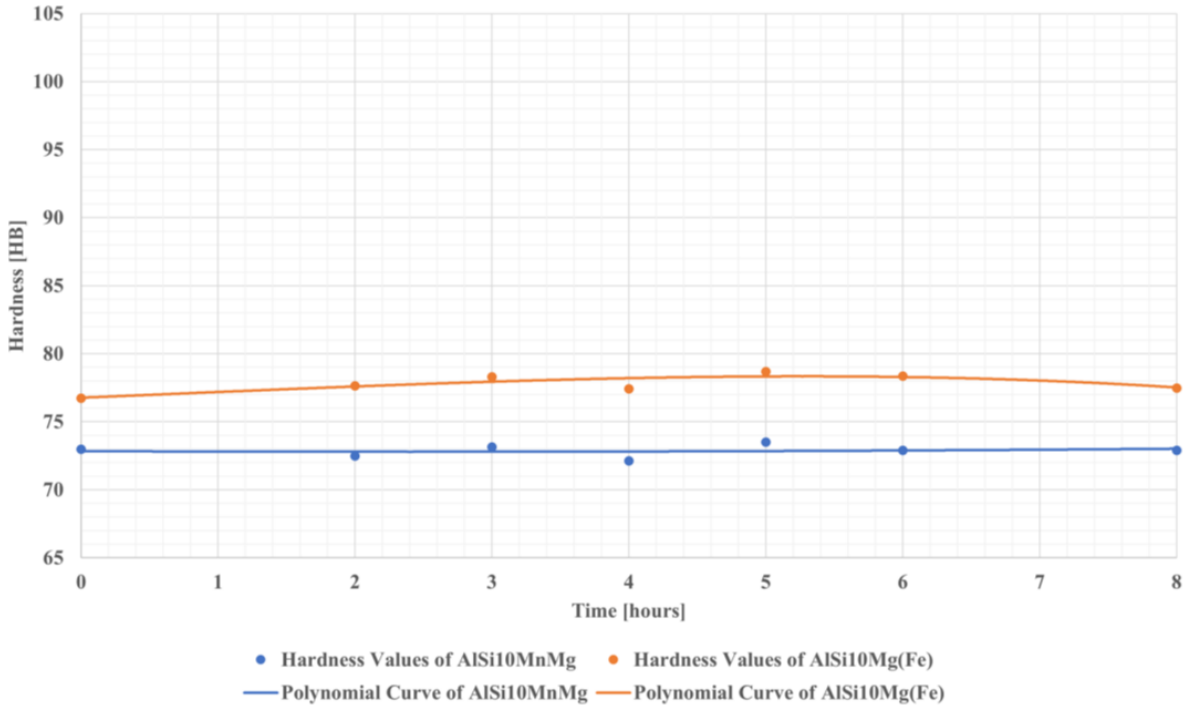

Figure 6. Hardness curves for heat treatment No. 2.

Contrary to what happened in heat treatment No. 1, both aluminium alloys did not respond to heat treatment No. 2. After the solution heat treatment (0 h in the graph of Figure 6), there was a decrease in hardness compared to the as-cast state. However, with artificial aging between 2 and 8 h, there is no significant variation in the hardness values

of the parts in both aluminium alloys. The low solution heat treatment temperature only promoted low or no dissolution of the elements in the aluminium matrix affecting the appearance and size of the precipitates upon artificial aging. The solution heat treatment time may also have been too short for the sufficient dissolution of elements in the aluminium matrix. However, the possible increase in hardness with the increase in solution heat treatment time does not justify the increase in energy consumption. All parts also had blisters.

In general, the standard deviations of the hardness values of the heat treatment No. 2 are lower than those from No. 1. This may be the result of the higher number and size of blisters with the solution heat treatment at 520 °C, which causes a higher occurrence of hardness measurements close to a blister. In addition, the parts with heat treatment No. 1 were more warped.

3.3. T5 Heat Treatments

The artificial aging stage time was 3 h for AlSi10MnMg alloy parts and 5 h for AlSi10Mg(Fe) alloy parts. These times are in accordance with the peak age hardening obtained in the T6 heat treatments with solution heat treatment No. 1.

Table 8 summarises the obtained hardness results.

Table 8. Hardness results in T5 heat treatments.

Artificial Aging at 180 °C	**Hardness [HB]**			
	AlSi10MnMg		**AlSi10Mg(Fe)**	
Time [h]	**Average**	**St. Deviation**	**Average**	**St. Deviation**
3	105	3.33	-	-
5	-	-	110	2.72
As-cast	87	2.04	89	1.08

The hardness values obtained for the AlSi10MnMg alloy parts are in agreement with [26], where the peak age hardening values after a T5 heat treatment are between 80 HB and 110 HB.

With the T5 heat treatment, higher hardness values were obtained when compared to the peak age hardening from the T6 heat treatment. This is more significant in the AlSi10Mg(Fe) alloy parts that have the highest hardness value (an increase of 10 HB between the T5 and T6 heat treatments). Furthermore, as in the T5 heat treatment, no solution heat treatment is performed, the parts are not subjected to high temperatures and do not present blisters. Hardness and blistering are crucial factors when deciding which heat treatment to perform on parts produced by vacuum-assisted HPDC for structural applications. Thus, the T5 heat treatment is recommended for these parts in these conditions, not only for the higher hardness values and no blistering, but also due to the reduction in energy consumption when compared to the T6 heat treatment (no-solution heat treatment).

3.4. Microstructural Characterisation

Figures 7–9 show the microstructures of the samples of both aluminium alloys used in the as-cast state and with T5 and T6 heat treatments, respectively.

There is no spheroidization of the silicon in either the as-cast or the T5 heat-treated samples, as these samples were not subjected to the solution heat treatment. The eutectic silicon is partially modified. Its morphology resembles lamellar and acicular structures.

A notable contrast emerges when comparing the microstructure of the T6 heat-treated samples with that of the as-cast and T5 heat-treated samples. In the former, silicon exhibits a more rounded shape. During the solution heat treatment, the eutectic silicon particles fragment, and the spheroidization of these particles takes place. Consequently, enhanced ductility is anticipated in these components.

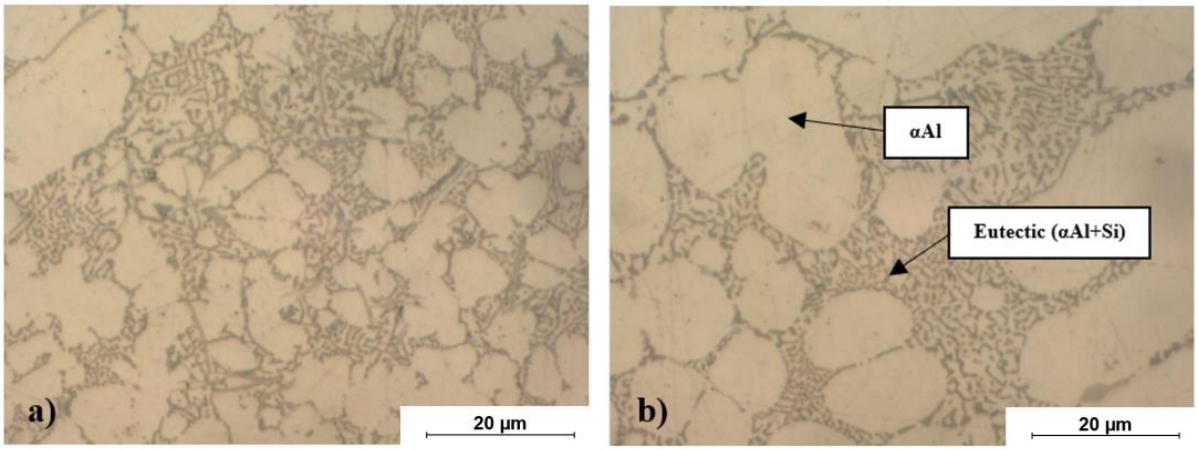

Figure 7. Microstructure of the alloy in the as-cast condition: (**a**) AlSi10Mg(Fe) alloy; (**b**) AlSi10MnMg alloy.

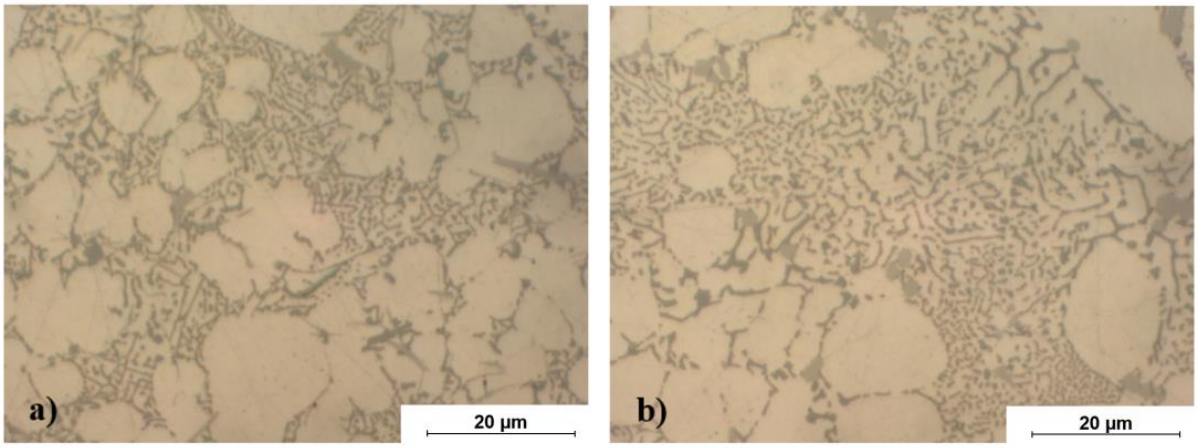

Figure 8. Microstructure of the alloy in the T5 heat treatment condition: (**a**) AlSi10Mg(Fe) alloy; (**b**) AlSi10MnMg alloy.

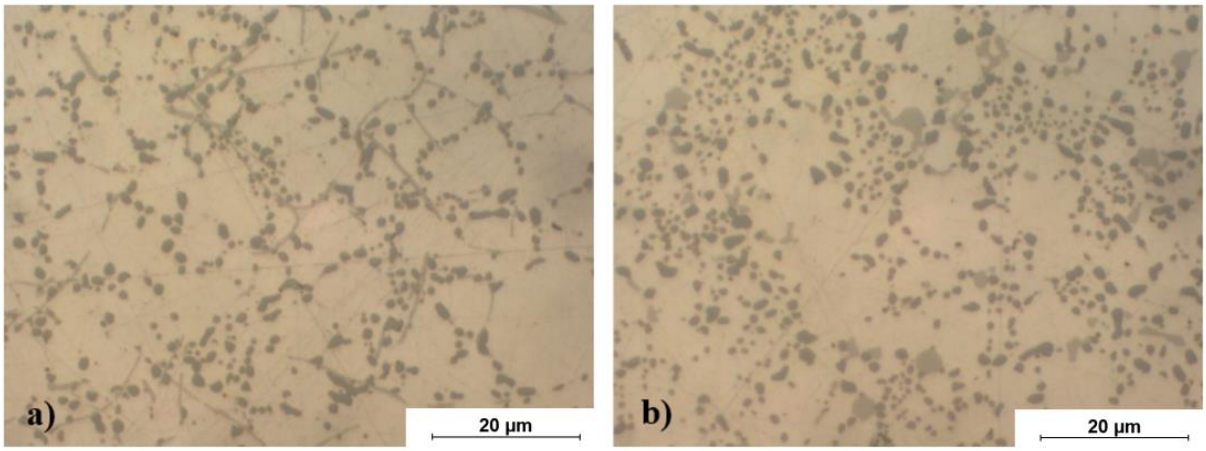

Figure 9. Microstructure of the alloy in the T6 heat treatment condition: (**a**) AlSi10Mg(Fe) alloy; (**b**) AlSi10MnMg alloy.

Figure 10 shows the main constituents present in the microstructure of AlSi10Mg(Fe) alloy in the as-cast state.

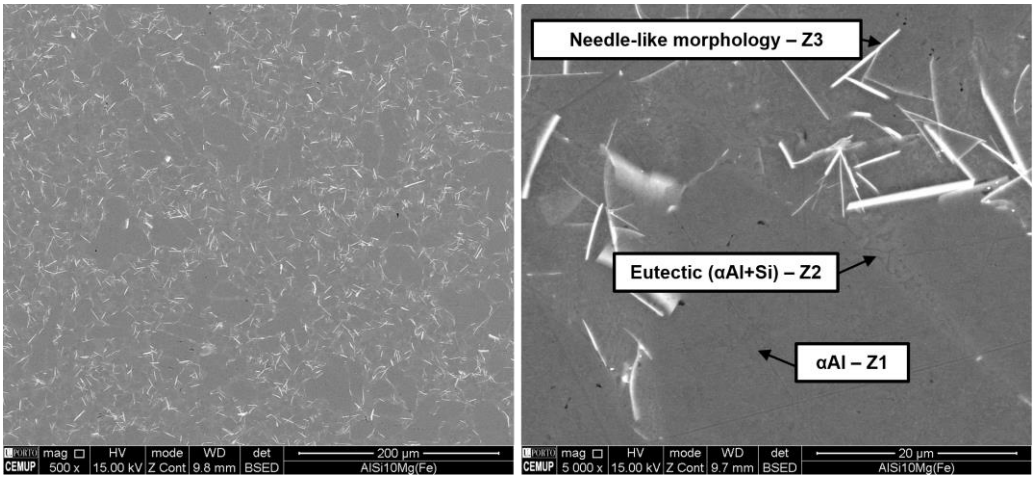

	Wt %		
Area	Al	Si	Fe
Z1	97.68	2.32	-
Z2	80.45	19.55	-
Z3	63.96	16.20	19.84

Figure 10. Microstructure of AlSi10Mg(Fe) alloy in the as-cast state.

It is possible to identify three different constituents: the primary aluminium phase (αAl), the eutectic silicon (αAl + Si), and a very bright needle-like morphology with a high percentage of iron. These needles are detrimental to ductility.

Considering that the AlSi10Mg(Fe) alloy is a secondary alloy produced from recycled aluminium, it is more sensitive to contamination, namely the appearance of lead in its chemical composition. This was also verified in the alloys' chemical composition analysis (Section 2.1).

The microstructure of the AlSi10MnMg alloy in the as-cast state is presented in Figure 11.

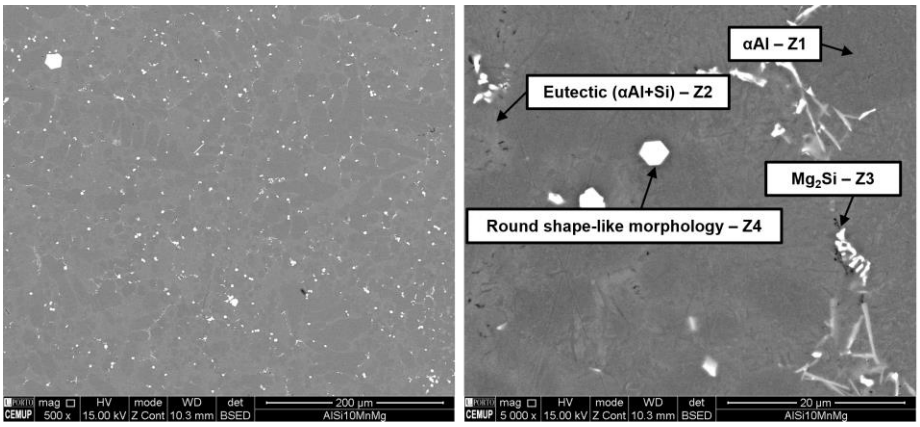

	Wt %				
Area	Al	Si	Fe	Mn	Mg
Z1	98.30	1.70	-	-	-
Z2	83.06	16.94	-	-	-
Z3	78.90	14.74	-	-	6.37
Z4	60.16	11.32	4.32	24.20	-

Figure 11. Microstructure of AlSi10MnMg alloy in the as-cast state.

Similar to the microstructure of AlSi10Mg(Fe) alloy, AlSi10MnMg alloy has the primary aluminium phase (αAl), the eutectic silicon (αAl + Si); however, it does not show the same bright needles proportion. Instead of these needles, bright small round-shaped morphologies appear, which is caused by the addition of manganese. The grey needles are composed mainly of magnesium. The dark spots are the Mg_2Si phase, a hardening phase.

Morphologies resembling Chinese scripts could also be observed (Figure 12). This type of morphology is typical of the AlSi10MnMg alloy due to the lower percentage of iron and the addition of manganese.

From Figures 10 and 11, there is a difference in the microstructure of aluminium alloys. The needles composed of iron are more prevalent in AlSi10Mg(Fe) alloy than in AlSi10MnMg alloy due to the higher amount of iron in its chemical composition. Thus, it is expected to obtain higher ductility values in AlSi10MnMg alloy parts.

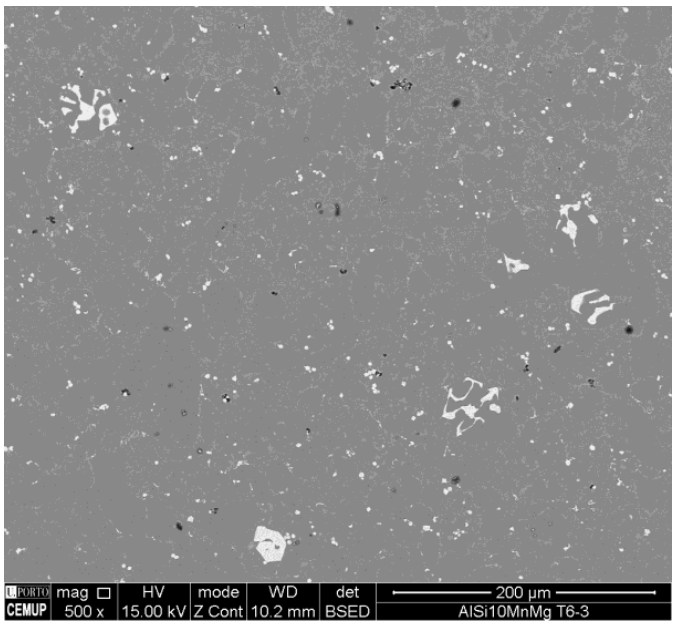

Figure 12. Chinese script-like morphology in AlSi10MnMg alloy T6 heat treated at the peak age hardening microstructure.

Figure 13 presents the skin's microstructure of both alloys. A refinement of the microstructure in the skin of both samples is observed. This occurs due to the high cooling rate, a typical characteristic of the HPDC process.

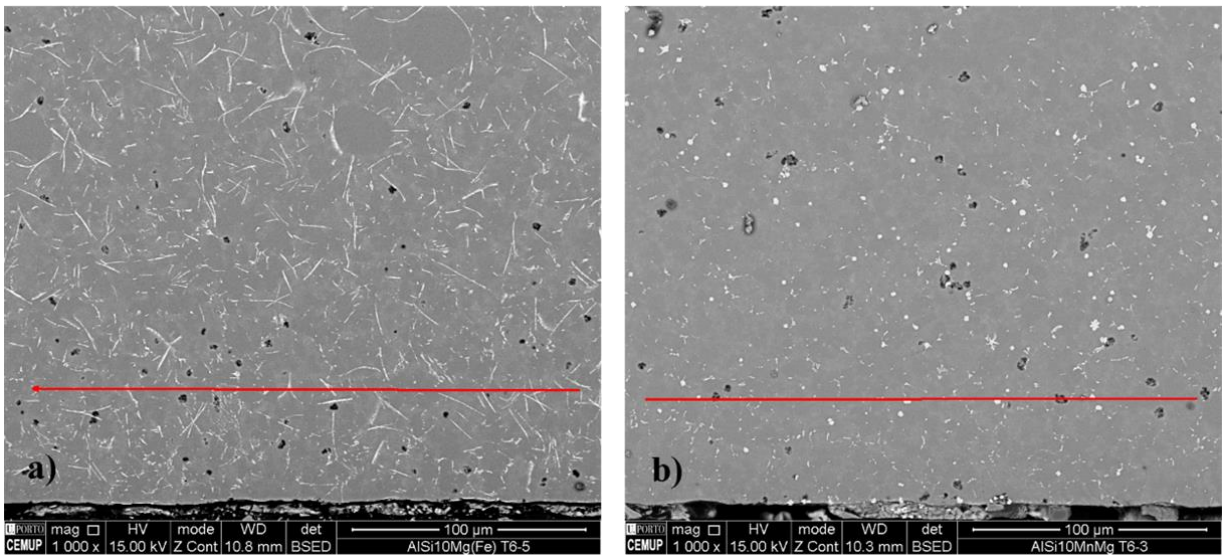

Figure 13. Microstructure of (**a**) AlSi10Mg(Fe) alloy, and (**b**) AlSi10MnMg alloy in the skin of the sample at the peak age hardening for T6 heat treatment.

3.5. Mechanical Characterisation

Each specimen was designated by its aluminium alloy (10—if made of AlSi10Mg(Fe) alloy and 36—if made of AlSi10MnMg alloy), by the part that it belongs to (1, 2, or 3) and, as there are three specimens in each part, they are also designated according to their position in the part from 1 to 3, as shown in the experimental procedure (Figure 2a). For example, the specimen designated as 10.1.2, is specimen No. 2 from part No. 1 of the AlSi10Mg(Fe) alloy. Some specimens were considered invalid during the tensile tests. Figure 14 shows the stress–strain curves of AlSi10Mg(Fe) alloy specimens.

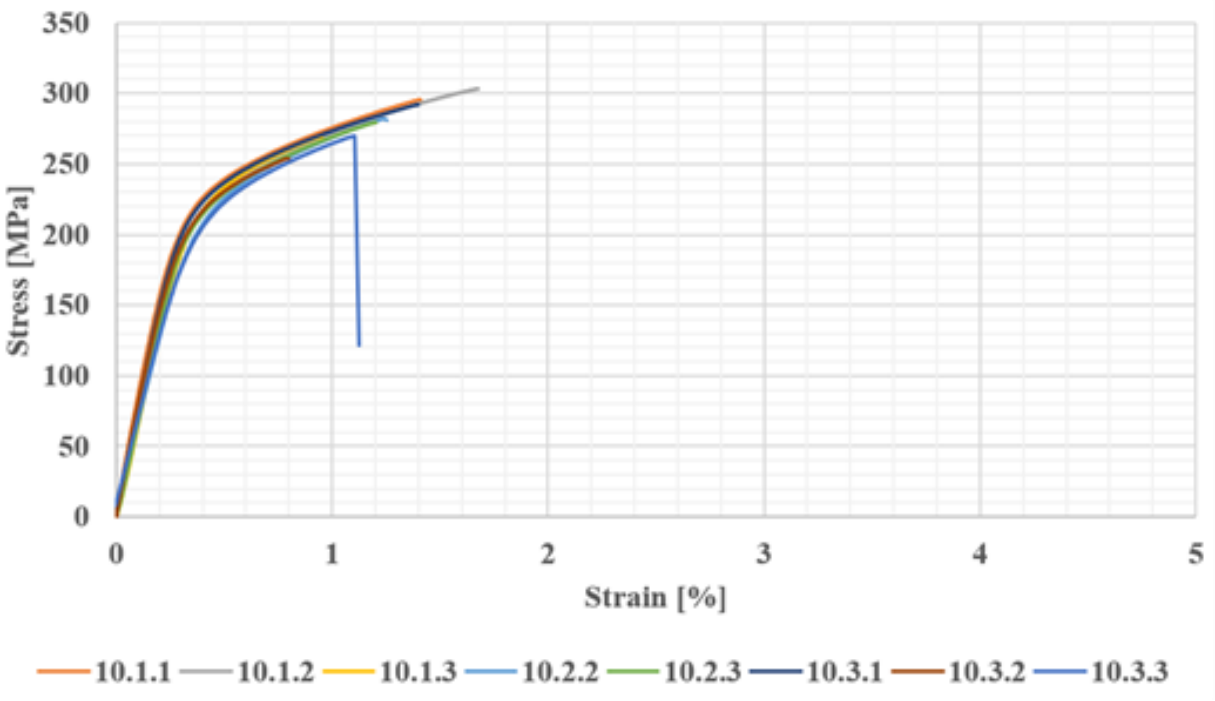

Figure 14. Stress–strain curves of AlSi10Mg(Fe) alloy specimens.

Figure 15 shows the stress–strain curves of the AlSi10MnMg alloy specimens.

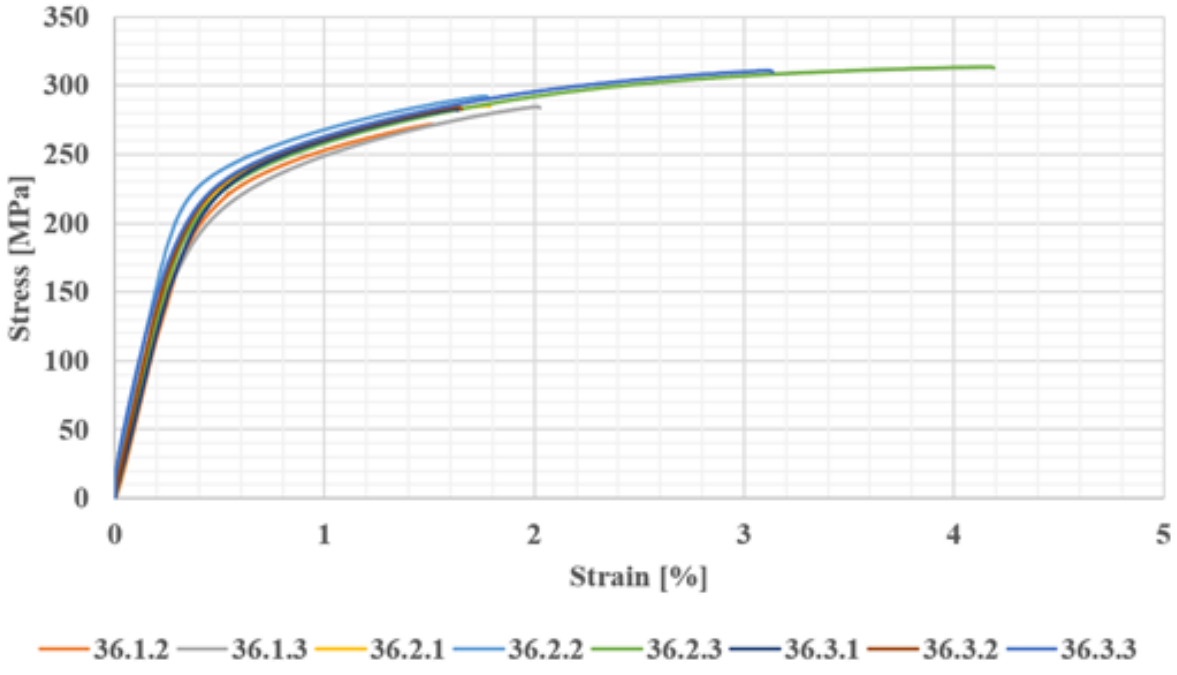

Figure 15. Stress–strain curves of AlSi10MnMg alloy specimens.

Specimens with the highest mechanical properties were at the extremities of the part in both aluminium alloys. This may be a result of the moulding design, where gas escape appears to have higher efficiency at the extremities.

Table 9 summarises the average values of the mechanical properties of these alloys in the as-cast state and after the T5 heat treatment.

Table 9. Mechanical properties of AlSi10Mg(Fe) and AlSi10MnMg alloys in as-cast and T5 state.

Alloy	State	$R_{p0.2}$ [MPa]	R_m [MPa]	A [%]
AlSi10Mg(Fe)	As-cast (1)	143	215	1.34
	T5	235	281	0.36
	As-cast (2)	>140	>240	>1
AlSi10MnMg	As-cast (1)	138	235	2.66
	T5	227	291	1.78
	As-cast (3)	120–150	250–290	5–11
	T5 (3)	155–245	275–340	4–9

1: values obtained from [24]; 2: values obtained from [27]; 3: values obtained from [26].

The effect of the T5 heat treatment on the parts is evident. The ultimate tensile strength demonstrates a remarkable rise, an increase of 31% in AlSi10Mg(Fe) alloy and of 24% in AlSi10MnMg alloy. The yield strength also experienced an increase, approximately 64% in both aluminium alloys. However, the ductility decreases by 36% in AlSi10Mg(Fe) alloy and 33% in AlSi10MnMg alloy. This goes in line with the expected effect of the T5 heat treatment, whose objective is to harden the heat-treated parts as much as possible.

The average yield strength value is slightly higher in the AlSi10Mg(Fe) alloy. However, the average ultimate tensile strength and elongation are higher in the AlSi10MnMg alloy. The secondary alloy, AlSi10Mg(Fe), has around 0.9% Fe, while the primary alloy, AlSi10MnMg, has roughly 0.1% Fe. Due to this higher percentage of iron, and as noted in Section 3.4, there is the formation of a higher quantity of β-AlFeSi phases in the AlSi10Mg(Fe) alloy, which has a needle-like morphology. This needle-like shape is detrimental to the mechanical properties, because when the alloy is dynamically tested these sharp morphologies are crack initiation sites that greatly reduce ductility. On the other hand, in the AlSi10MnMg alloy, as the percentage of iron is reduced and manganese is added, there is a higher predominance of α-AlFeMnSi phases compared to β phases. The morphology of the alpha phases is more rounded, which does not make them crack initiation sites, and therefore there is an improvement in the ductility of the primary alloy. Nevertheless, the ductility remains low in both aluminium alloys and this may be a result of the high levels of porosity in the tested parts.

4. Conclusions

In summary, this study highlights the following main points:

1. Solution heat treatments conducted at temperatures ranging from 360 °C to 520 °C for 15 min or more resulted in the formation of blisters.
2. Despite the use of the injection process with vacuum assistance, it was not sufficient to reduce the porosity level to a degree that could prevent blistering.
3. The solution heat treatment temperature appears to have a greater influence on the appearance of blisters than the solution heat treatment time.
4. A solution heat treatment at 360 °C for 30 min followed by several artificial aging steps at 180 °C between 2 h and 8 h had no effect on the parts' hardness.
5. The T5 heat treatment appears to be the most suitable for these parts in such conditions. Not only does it prevent the blisters' appearance, but it also obtains better hardness values and reduces energy consumption due to the absence of the solution heat treatment when compared to the T6 heat treatment.
6. The solution heat treatment promoted the spheroidization of the silicon particles.
7. With the T5 heat treatments, an increase in ultimate tensile strength and yield strength was obtained. However, ductility and toughness values suffered a decrease in both aluminium alloys.

Author Contributions: Conceptualization, G.S., R.M., R.P.S., R.N. and A.R.; methodology, R.G., G.S. and R.M.; software, R.G., G.S. and R.M.; validation, G.S., R.M., R.P.S. and R.N.; investigation, R.G., G.S., R.M., J.S., R.P.S. and C.F.; writing—original draft preparation, R.G. and G.S.; writing—review

and editing, G.S., J.S., R.P.S., C.F. and A.R.; supervision, R.M. and R.N.; project administration, R.P.S. and A.R.; funding acquisition, A.R. All authors have read and agreed to the published version of the manuscript.

Funding: Authors gratefully acknowledge the funding of Project Hi-rEV—Recuperação do Setor de Componentes Automóveis (C644864375-00000002), co-financed by Plano de Recuperação e Resiliência (PRR), through NextGeneration EU.

Data Availability Statement: The original contributions presented in the study are included in the article, further inquiries can be directed to the corresponding author.

Acknowledgments: The authors would like to acknowledge the members of Project Hi-rEV—Recuperação do Setor de Componentes Automóveis, namely Palbit S.A. for their technical support.

Conflicts of Interest: Author Cristina Fernandes was employed by the company Palbit S.A. The remaining authors declare that the research was conducted in the absence of any commercial or financial relationships that could be construed as a potential conflict of interest.

References

1. MacKenzie, D.S.; Totten, G.E. *Handbook of Aluminum*; CRC Press: Boca Raton, FL, USA, 2003. [CrossRef]
2. BIR. Non-Ferrous Metals. 2023. Available online: https://www.bir.org/the-industry/non-ferrous-metals (accessed on 11 June 2024).
3. Luo, A.A.; Sachdev, A.K.; Apelian, D. Alloy development and process innovations for light metals casting. *J. Mater. Process. Technol.* **2022**, *306*, 117606. [CrossRef]
4. Czerwinski, F. Current Trends in Automotive Lightweighting Strategies and Materials. *Materials* **2021**, *14*, 6631. [CrossRef] [PubMed]
5. Stojanovic, B.; Epler, I. Application of aluminum and aluminum alloys in engineering. *Appl. Eng. Lett.* **2018**, *3*, 52–62. [CrossRef]
6. Musfirah, A.; Jaharah, A. Magnesium and aluminum alloys in automotive industry. *J. Appl. Sci. Res.* **2012**, *8*, 4865–4875.
7. Monteiro, F.; Soares, G.; Madureira, R.; Silva, R.P.; Silva, J.; Amaral, R.; Neto, R.; Reis, A.; Esteves, A. Development of the Low-Pressure Die Casting Process for an Aluminium Alloy Part. *Materials* **2024**, *17*, 2835. [CrossRef] [PubMed]
8. Hartlieb, M. Aluminum alloys for structural die casting. *Die Cast. Eng.* **2013**, *57*, 40–43.
9. Watson, D. Microstructure and Mechanical Properties of Ductile Die-Cast AlMgSi-Mn Alloys. Ph.D. Thesis, Brunel University, London, UK, 2015; p. 169.
10. Casarotto, F.; Franke, A.J.; Franke, R. High-pressure die-cast (HPDC) aluminium alloys for automotive applications. In *Advanced Materials in Automotive Engineering*; Rowe, J., Ed.; Elsevier: Amsterdam, The Netherlands, 2012; Chapter 6; pp. 109–149. [CrossRef]
11. Franco, B.; Gramegna, N.; Timelli, G. High-Pressure Die-Casting: Contradictions and Challenges. *JOM* **2015**, *67*, 901–908. [CrossRef]
12. Beeley, P. *Foundry Technology*; Elsevier Science: Amsterdam, The Netherlands, 2001.
13. De Carvalho Ferreira, J.M.G. *Tecnologia da Fundição*; Fundação Calouste Gulbenkian: Lisboa, Portugal, 1999.
14. Andresen, W. *Die Cast Engineering: A Hydraulic, Thermal, and Mechanical Process*; CRC Press: Boca Raton, FL, USA, 2004.
15. Martins, M.M.M. Estudo do Comportamento das Ligas de Alumínio 6061 e 6082. Master's Thesis, Universidade de Aveiro, Aveiro, Portugal, 2008.
16. Kaufman, J.G.; Rooy, E.L. *Aluminum Alloy Castings: Properties, Processes, and Applications*; American Foundry Society: Cleveland, OH, USA; ASM International: Almere, The Netherlands; Schaumburg, IL, USA, 2004.
17. Mohamed, A.M.A.; Samuel, F.H. A Review on the Heat Treatment of Al-SiCu/Mg Casting Alloys. In *Heat Treatment—Conventional and Novel Applications*; InTech: Rijeka, Croatia, 2012; Chapter 4. [CrossRef]
18. Hu, X.G.; Zhu, Q.; Midson, S.P.; Atkinson, H.V.; Dong, H.B.; Zhang, F.; Kang, Y.L. Blistering in semi-solid die casting of aluminium alloys and its avoidance. *Acta Mater.* **2017**, *124*, 446–455. [CrossRef]
19. Rheinfelden Alloys. Primary Aluminium Alloys for Pressure Die Casting. 2016. Available online: https://rheinfelden-alloys.eu/wp-content/uploads/2017/01/Handbook-Die-Casting-Aluminium-Alloys_RHEINFELDEN-ALLOYS_2016_EN.pdf (accessed on 30 May 2024).
20. Cai, Q.; Mendis, C.L.; Chang, I.T.H.; Fan, Z. Effect of short T6 heat treatment on the microstructure and the mechanical properties of newly developed die-cast Al–Si–Mg–Mn alloys. *Mater. Sci. Eng. A* **2020**, *788*, 139610. [CrossRef]
21. Kang, H.-J.; Park, J.-Y.; Choi, Y.-S.; Cho, D.-H. Influence of the Solution and Artificial Aging Treatments on the Microstructure and Mechanical Properties of Die-Cast Al–Si–Mg Alloys. *Metals* **2022**, *12*, 71. [CrossRef]
22. Kang, H.-J.; Jang, H.-S.; Yoon, P.-H.; Lee, G.-H.; Park, J.-Y.; Kim, E.S.; Choi, Y.S. Effects of solution treatment temperature and time on the porosities and mechanical properties of vacuum die-casted and T6 heat-treated Al-Si-Mg alloys. *Vacuum* **2021**, *193*, 110536. [CrossRef]
23. Lumley, R.N.; Polmear, I.J.; Curtis, P.R. Rapid Heat Treatment of Aluminum High-Pressure Diecastings. *Met. Mater. Trans. A* **2009**, *40*, 1716–1726. [CrossRef]

24. Soares, G.; Neto, R.; Madureira, R.; Soares, R.; Silva, J.; Silva, R.P.; Araújo, L. Characterization of Al Alloys Injected through Vacuum-Assisted HPDC and Influence of T6 Heat Treatment. *Metals* **2023**, *13*, 389. [CrossRef]
25. *ASTM B557M-15*; Standard Test Methods for Tension Testing Wrought and Cast Aluminum- and Magnesium-Alloy Products (Metric). ASTM International: West Conshohocken, PA, USA, 2016.
26. Silafont—An Infinite Wealth of Properties. *Rheinfelden*. 2021. Available online: https://rheinfelden-alloys.eu/en/alloys/silafont/ (accessed on 9 June 2024).
27. *NP EN1706*; Alumínio e Ligas de Alumínio. 2000. Available online: https://biblioteca.isel.pt/cgi-bin/koha/opac-detail.pl?biblionumber=19990 (accessed on 9 June 2024).